Original Article
Utility of intravoxel incoherent motion diffusion-weighted imaging in differentiating renal cell carcinoma from angiomyolipoma

Congrui Li[1*], Yan Liu[1*], Xiaoping Yu[1], Yu Xie[2], Yan Sun[1]

[1]Department of Diagnostic Radiology, Hunan Cancer Hospital, The Affiliated Cancer Hospital of Xiangya School of Medicine, Central South University, Changsha, Hunan, China; [2]Department of Urological Surgery, Hunan Cancer Hospital, The Affiliated Cancer Hospital of Xiangya School of Medicine, Central South University, Changsha, Hunan, China. *Equal contributors.

Abstract: We discussed the utility of intravoxel incoherent motion diffusion-weighted imaging (IVIM-DWI) for discriminating clear cell renal cell carcinoma (ccRCC) from angiomyolipoma (AML). Preoperative IVIM-DWI parameter (ADC,D, D and f) values were compared between the ccRCC (n = 37) and AML (n = 28) groups. AML exhibited significantly lower ADC ([1.35±0.29] × 10^{-3} mm^2/s vs [1.77 ± 0.41] × 10^{-3} mm^2/s) and D ([0.90±0.34] × 10^{-3} mm^2/s vs [1.36±0.31] × 10^{-3} mm^2/s) values (all P<0.001), whereas obviously higher D* value ([18.06 ± 7.49] × 10^{-3} mm^2/s vs [14.15±4.70] × 10^{-3} mm^2/s) (P<0.05) than ccRCC. Optimal cut-off values (area under the curve, sensitivity and specificity) for distinguishing ccRCC from AML were as follows: ADC = 1.54 × 10^{-3} mm^2/s (0.804, 78.57% and 81.08%), D = 0.83 × 10^{-3} mm^2/s (0.850, 64.29% and 100.00%), and D* = 20.53 × 10^{-3} mm^2/s (0.647, 32.14% and 100.00%). Both the diffusion- and perfusion-related IVIM-DWI parameters may be helpful in differentiating ccRCC from AML.

Keywords: Intravoxel incoherent motion, diffusion-weighted imaging, renal tumor, sensitivity and specificity

Introduction

Comprising 85%-90% of renal malignancies, renal cell carcinoma (RCC) is the most common primary malignant tumor of the kidney [1, 2]. Angiomyolipoma (AML), the most frequent benign tumor of the kidney, accounts for 7%-9% of renal tumors [2]. Accurately discriminating the two types of neoplasms is essential for determining an appropriate treatment and predicting the prognosis for patients with renal tumor. Nowadays, imaging approaches such as computed tomography (CT) and magnetic resonance imaging (MRI) play important roles in preoperatively identifying the pathological nature of renal tumors. The differential diagnosis between AML and RCC is always not difficult because AML usually exhibits significant fat on plain CT and MRI. However, such differentiation may be hard to make for AML with little or no visible fat, especially for those in small size. Although contrast-enhanced CT and MRI can

benefit such differentiation [3-6], they are associated with some shortages including radiation injury, allergic reactions to contrast agent, contrast-induced nephropathy (CIN) and/or nephrogenic systemic fibrosis (NSF), which limits their clinical applications.

Previous studies suggested that AML differs significantly from RCC in the value of apparent diffusion coefficient (ADC) derived from diffusion-weighted MRI (DWI),a non-invasive MRI technique able to quantitate the diffusion motion of water molecule in tissues [2, 7]. Additionally, dynamic contrast-enhanced CT (DCE-CT) and MRI (DCE-MRI) demonstrated obvious differences in the microcirculation perfusion between these two common renal tumors [3-5]. Recently, intravoxel incoherent motion DWI (IVIM-DWI) has gained significantly increasing attention because of its ability to simultaneously quantitate water molecular diffusion and microcirculation perfusion in viable tissues,

Table 1. Characteristics of patients and tumors

Parameters	AML (n = 28)	ccRCC (n = 37)	P value
Age (years)	50.14 ± 11.01	54.22 ± 10.78	0.082
Long diameter (mm)	50.18 ± 34.81	54.22 ± 20.59	0.074
Gender			0.413
Male	13	21	
Female	15	16	
Location			0.188
Right Kidney	12	22	
Left Kidney	16	15	

AML, angiomyolipoma; ccRCC, clear cell renal cell carcinoma.

Table 2. Comparisons of the IVIM-DWI parametric values (mean ± standard deviation) between the AML and ccRCC groups

Parameters	AML (n = 28)	ccRCC (n = 37)	P value
ADC (× 10^{-3} mm²/s)	1.35 ± 0.29	1.77 ± 0.41	0.000
D (× 10^{-3} mm²/s)	0.90 ± 0.34	1.36 ± 0.31	0.000
D* (× 10^{-3} mm²/s)	18.06 ± 7.49	14.15 ± 4.70	0.044
f	0.40 ± 0.11	0.38 ± 0.16	0.070

IVIM-DWI, intravoxel incoherent motion diffusion-weighted imaging; AML, angiomyolipoma; ccRCC, clear cell renal cell carcinoma; ADC, apparent diffusion coefficient; D, pure diffusion coefficient; D*, pseudo-diffusion coefficient; f, perfusion fraction.

without the administration of exogenous contrast agent. This new MRI approach is reportedly helpful in tumor diagnosis, for example characterizing benign and malignant pancreatic masses [8], distinguishing non-metastatic from metastatic lymph node in rectal carcinoma [9], and identifying pathological subtype of renal cancer [10]. Nevertheless, the utility of IVIM-DWI in the differential diagnosis between AML and RCC has not been well understood. Thus, the purpose of this study was to investigate the diagnostic value of IVIM-DWI in distinguishing these two types of the most common renal tumors.

Materials and methods

Patients and Histopathology

This single-center, retrospective study was conducted in accordance with the declaration of Helsinki and with approval from the Medical Ethics Committee of our institution. Written informed consent was obtained from all patients. From December 2014 to March 2015, 67 patients with renal AML or clear cell RCC (ccRCC) were collected. All patients underwent pre-operative IVIM-DWI plus conventional MRI,

and they did not receive any prior anti-tumor treatment. After surgery, the tumor specimen was reviewed by an experienced pathologist and the histopathological type of the resected renal tumors was subsequently determined. Of the 67 patients who were initially enrolled, 2 were excluded because of poor IVIM-DWI imaging quality. Thus, the present study eventually included 28 cases of AML and 37 cases of ccRCC. All the AML and ccRCC belong to solitary lesion. The characteristics of the patients and tumors are presented in **Table 1**.

MRI protocols

All MRI examinations were performed on a 1.5-Tesla MRI scanner (Optima MR-360, GE Healthcare, Waukesha, WI, USA) with a phased-array body coil. The patients were trained to breathe deeply prior to holding their breath, and their abdominal wall was secured in front of the coil by using a bandage in order to reduce motion artifacts during MRI data acquisition.

The conventional MRI protocols included the following sequences: 1) axial T1-weighted dual-echo in-phase and out-of-phase sequence: (number of slice 24, 205-ms time of repetition [TR], 2.1/4.2-ms time of echo [TE], 4-mm slice thickness, 1-mm slice space, field of view [FOV] 380 × 342 mm, acquisition matrix of 256 × 160, number of excitations [NEX] of 1) ; 2) axial T2-weighted fast spin-echo (FSE) images with fat suppression (number of slice 24, 6000-ms TR, 86.4-ms TE, 4-mm slice thickness, 1-mm slice space, FOV 380 × 342 mm, acquisition matrix of 320 × 192, number NEX of 2); 3) axial and coronal T1-weighted fast spoiled gradient echo (FSPGR) contrast-enhanced images with fat suppression (number of slice 24, 165-ms TR, 2.3-ms TE, 4-mm slice thickness, 1-mm slice space, FOV 400 × 400 mm, acquisition matrix of 384 × 192, number NEX of 2). The contrast agent gadodiamide (Omniscan®, GE Healthcare) was administered intravenously at a dose of 0.1 mmol/kg of body weight.

IVIM-DWI was performed before the administration of gadodiamide. Twelve b values (0, 20, 30, 50, 80, 100, 150, 200, 400, 600, 800 and 1000 s/mm²) were applied with a single-shot
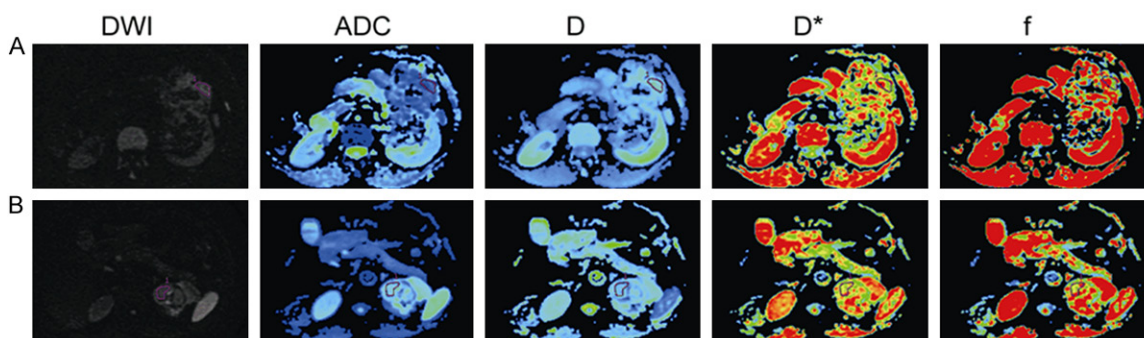
Figure 1. Images in Row A and B are axial DWI (b=600 s/mm^2) and IVIM-DWI parametric maps of an AML and a ccRCC, respectively. The ADC, D, D* and *f* values for AML were 1.21 × 10^{-3} mm^2/s, 0.59 × 10^{-3} mm^2/s, 18.80 × 10^{-3} mm^2/s and 0.375, respectively. The ADC, D, D* and *f* values for ccRCC were 1.87 × 10^{-3} mm^2/s, 1.35 × 10^{-3} mm^2/s, 14.10 × 10^{-3} mm^2/s and 0.396, respectively. DWI, diffusion-weighted imaging; IVIM-DWI, intravoxel incoherent motion diffusion-weighted imaging; AML, angiomyolipoma; ccRCC, clear cell renal cell carcinoma; ADC, apparent diffusion coefficient; D, pure diffusion coefficient; D*, pseudo-diffusion coefficient; *f*, perfusion fraction.

Table 3. Optimal cut-off IVIM-DWI parametric values for differentiating AML from ccRCC based on receiver operating characteristic curve analysis

Parameters	Cut-off value	AUC (95% CI)	Sensitivity	Specificity	*P* value
ADC	1.54 × 10^{-3} mm^2/s	0.804 (0.687-0.892)	78.57%	81.08%	0.291[a]
D	0.83 × 10^{-3} mm^2/s	0.850 (0.740-0.927)	64.29%	100.00%	0.004[b,#]
D*	20.53 × 10^{-3} mm^2/s	0.647 (0.517-0.760)	32.14%	100.00%	0.072[c]

IVIM-DWI, intravoxel incoherent motion diffusion-weighted imaging; ccRCC, clear cell renal cell carcinoma; AML, angiomyolipoma; AUC, area under the curve; CI, confidence interval; ADC, apparent diffusion coefficient; D, pure diffusion coefficient; D*, pseudo-diffusion coefficient. a, ADC vs D; b, D vs D*; c, D* vs ADC; #significance after Bonferroni-correction (P<0.05/3).

diffusion-weighted spin-echo echo-planar sequence. The lookup table of gradient direction was modified to allow multiple-b-value measurements in one series. Parallel imaging was used with an acceleration factor of 2. In total, 20 axial slices covering the kidney region were obtained with an FOV of 380 × 304 mm, 4-mm slice thickness, 1-mm slice gap, 6000-ms TR, 81.7-ms TE, matrix of 128 × 130, and NEX of 4.

IVIM-DWI analysis

All IVIM-DWI data were imported into the Advantage Workstation with FuncTool software (version AW 4.6, GE Healthcare) for post-processing. The IVIM-DWI data were independently and double-blindly evaluated by two radiologists (L.Y. and Y.X., with 15 and 20 years of experience in abdomen radiology, respectively). The main principle and procedures of the IVIM-DWI analysis were described previously [11, 12]. Briefly, according to the formula $S_b/S_0 = (1 - f)$ exp(-b D) + f exp (-b D*), where S_b is the signal intensity with diffusion gradient b (b ≠ 0 s/mm^2), S_0 is the signal intensity for the b value of 0 s/mm^2, D is the true diffusion coefficient

indicating the pure diffusion of the water molecule, D* is the pseudo-diffusion coefficient demonstrating microcirculation perfusion, and *f* is the microvascular volume fraction representing the fraction of diffusion related to microcirculation perfusion. The ADC value was generated from the formula S_b/S_0 = exp (-b D) based on conventional DWI with the MRI data at high b values (200, 400, 600, 800 and 1000 s/mm^2).

The regions of interest (ROIs) were manually drawn in the tumor parenchyma. Six ROIs were manually drawn by each observer for each tumor on its DWI images (b=600 s/mm^2) at least 3 sections, using conventional axial T1-weighted, T2-weighted and contrast-enhanced images as references. Care was taken to avoid the inclusion of visual cystic, necrotic, large vessels, hemorrhage and fat areas. The ROIs were subsequently propagated to the IVIM-DWI parametric maps for measuring the metric values. For each parameter, 12 numerical values were generated totally by the two observers for each lesion. The final value for each parameter was designated as the mean value of the 12
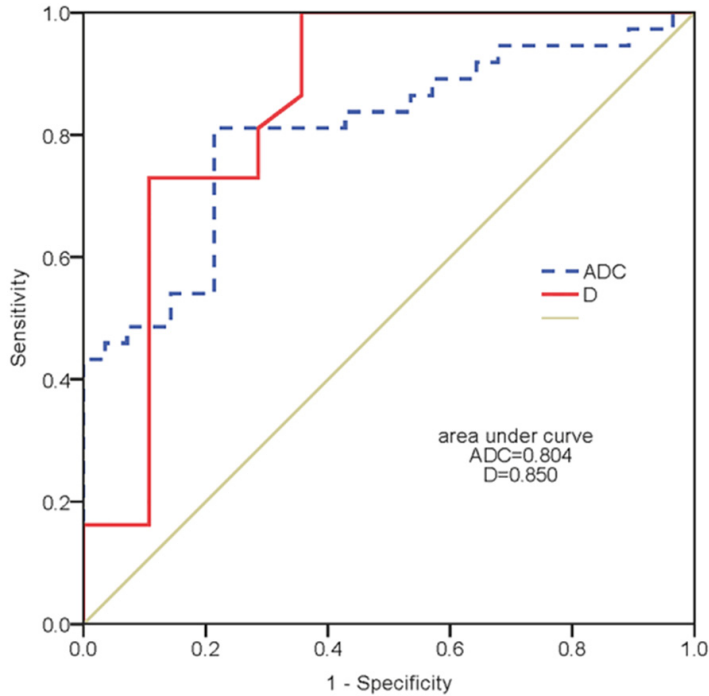
Figure 2. The diagnostic accuracy of ADC and D in differentiating angiomyolipoma from clear cell renal cell carcinoma.
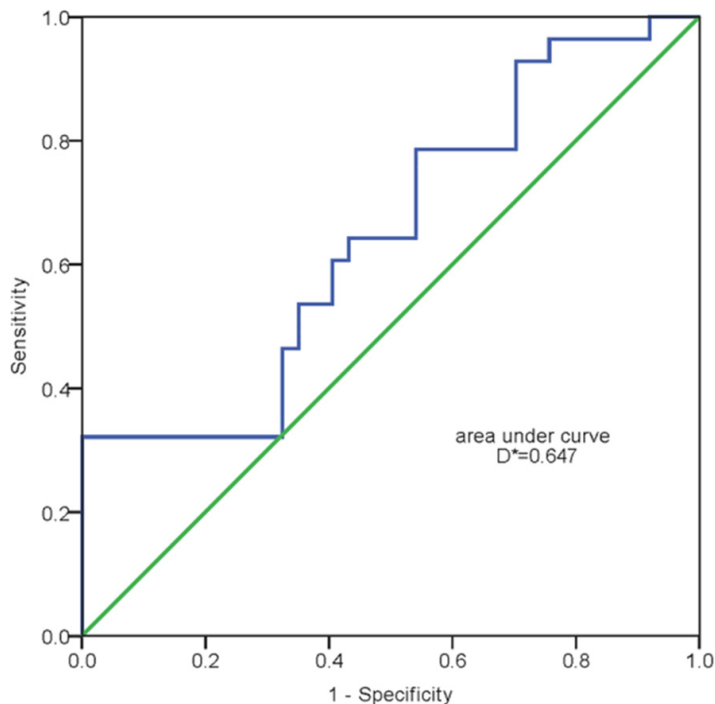
Figure 3. The diagnostic accuracy of D* in differentiating angiomyolipoma from clear cell renal cell carcinoma.

numerical values above. The average size of the ROIs was 77.21 ± 42.84 mm^2 (range, 37-

203 mm^2) for AML and 140.97 ± 51.32 mm^2 (range, 35-234 mm^2) for ccRCC, respectively.

Statistical analysis

The IVIM-DWI parametric values for the AML and ccRCC groups were expressed as mean ± standard deviation, and analyzed using SPSS v19.0 (IBM Corporation, Armonk, NY, USA) or MedCalc v15.0 (MedCalc Software bvba, Ostend, Belgium). *P* values less than 0.05 were considered statistically significant. Non-parametric Mann-Whitney U test was used to compare the differences in the IVIM-DWI metric values, lesion size and age between these two groups. Chi-squared test was performed to test the differences in the gender and tumor location between the AML and ccRCC groups. Receiver operating characteristic (ROC) curves were generated for each parameter with statistically significant difference in order to determine the optimal cut-off value resulting in the best possible diagnostic accuracy according to the Youden Index.

Results

The IVIM-DWI parametric values for the renal tumors are summarized in **Table 2**. **Figure 1** shows representative images of AML and ccRCC. AML exhibited significantly lower ADC and D values (all *P*< 0.001), together with higher D* value (*P*<0.05), than ccRCC. The two types of renal tumors shared similar *f* values (*P* = 0.070). In identifying AML from ccRCC based on ROC curve analysis, the area under the curve (AUC) value for D (0.850) was the highest, followed by that for ADC, whereas D* had the lowest AUC value (**Table 3**; **Figures 2** and **3**).

Discussion

Accounting for about 70% of all RCC, ccRCC has relatively more aggressive behavior and worse

prognosis than non-ccRCC including papillary and chromophobe subtypes [13]. In addition, ccRCC and non-ccRCC always exhibit distinctly different imaging appearances on diffusion- and/or perfusion-related MRI approaches such as IVIM-DWI and DCE-MRI [14-16]. This suggests that there are obvious differences in tissue features, including tumor vascularity and/or cellularity/architecture, between ccRCC and non-ccRCC. In view of the possibility that these differences might negatively influence the diagnostic utility of IVIM-DWI in separating AML and RCC, non-ccRCC was excluded from the present study. Therefore, this study mainly focused on the discrimination between the most common renal tumors (ccRCC and AML), and demonstrated that both the diffusion- and perfusion-related IVIM-DWI parameters benefit this differential diagnosis.

According to the IVIM theory [17], both D* and f are perfusion-related parameters. D* is proportional to the average blood velocity and the mean capillary segment length [17, 18]. Being the ratio of the volume occupied by the MRI-detectable water in the capillary networks [17, 18], f depends mainly on the microvessel attenuation of tissues. In this study, AML exhibited obviously higher D* value than ccRCC. This finding might suggest that average blood velocity and/or capillary segment length in AML are higher and/or larger than those in ccRCC. It is usually considered that tumor vessels are tortuous with irregular branches in a chaotic network of tangles, and the higher the tumor malignancy degree is, the more tortuous and chaotic its vessels are. Compared with ccRCC, the vessels in AML may be less tortuous and chaotic, which means that AML has longer capillary segment length and subsequently higher blood velocity. This opinion could be partly supported by previous observations that AML shows a significantly higher relative enhancement in the arterial phase on multiphasic contrast-enhanced MRI [15, 16]. In line with a recent report [10], AML did not differ significantly from ccRCC in the f value in the present study, which indicates that there may be not distinct difference in the micro-vessel attenuation between these two renal tumors. This finding may be interpreted by a widely accepted opinion that both AML and ccRCC are rich in tumor vessels, which usually results in obvious enhancement for both the two renal tumors on DCE-CT or DCE-MRI. Of note, the measurement of the f value was found to be greatly dependent on a variety of factors such as the T2 relaxation time of tissue, the TE time and the number of b value for IVIM-DWI data acquisition [19, 20]. Considering that the difference in the f value between AML and ccRCC in this study almost approached statistical significance, there may be a possibility that some technical factors and tissue characteristics may limit the efficacy of IVIM-DWI in detecting the possible differences in microvessel attenuation between these two tumors.

Based on the IVIM theory [17], D reflects the pure diffusion (i.e., the Brownian motion) of water molecule. Being a combination of D and D*, ADC reflects the total diffusion of water molecule and primarily depends on D when the b value is higher than 200 s/mm^2. Thus, ADC is mainly a diffusion-related parameter at high b value. Pathologically, AML is composed of smooth muscle, fat-containing cells and thick-walled blood vessels with characteristic bundles of smooth muscle emanating from the vessel walls. Compared with ccRCC, the relatively lower ADC and D values for AML in the present study can be explained by its rich components of muscle and fat that restrict diffusion motion of water molecule [21]. Another possible reason for the relatively higher ADC and D values for ccRCC may be the micronecrosis and/or microcystic change possibly confirmed by pathologic examination rather than on MRI images. Although visible necrosis and cystic change were excluded from ROIs when we measured the IVIM-DWI parametric values in this study, it was almost impossible to avoid the inclusion of these microscopical necrosis and cystic degeneration into ROIs. Generally speaking, necrosis and cystic degeneration more easily occur in ccRCC than in AML. In regard to the ADC value for AML and ccRCC, our observations are in agreement with several prior reports [22-25], whereas inconsistent with some previous studies [2, 7, 26] in which AML had higher ADC value than ccRCC. These inconsistent observations suggest that the utility of ADC in discriminating AML from ccRCC may be limited. It may depend on the size of tumor, pathological components of tumor (for example the variable proportion of fat, smooth muscle and blood vessels in AML), imaging protocols, methods for DWI data analysis (such as the placement of ROIs) and so on.

As for D, it had the highest AUC value of 0.850, along with the highest specificity of 100.00%, among all the IVIM-DWI parameters in the differentiation between AML and ccRCC in the present study. Furthermore, this study demonstrated that the difference in the AUC value of ROC curve between D and D* reached statistical significance. These findings may suggest that the diffusion of water molecule is a more important micro-environmental characteristic of tumor tissue than the microcirculation perfusion in differentiating AML from ccRCC. Apart from our findings, a recent study also found that the D value for AML is obviously lower than that for ccRCC [10]. Therefore, D may serve as an important imaging marker for identifying these two common renal tumors. Nevertheless, the exact differentiation efficacy of D is not entirely clarified and deserves further investigation because few published reports are currently available.

Our study had several limitations. Firstly, the retrospective nature and relatively small patient cohort of this study may result in statistical bias. Secondly, the fat-rich and fat-poor AML were analyzed as a whole in the present study because of the limited number of fat-poor AML due to its low prevalence, which may have negative influence on our results. In this study, we carefully avoided the inclusion of fat-containing area into ROIs as possible as we can. Our findings might help the readers better understand the differences in the perfusion- and diffusion-related micro-environments between AML and ccRCC, and therefore might serve as a potential reference with respect to differentiating ccRCC from fat-poor AML. Thirdly, the IVIM analysis in our study was based on drawing ROIs that covered part areas of renal tumors to investigate their mean parametric values. It is well known that tumor often exhibits histological heterogeneity. Therefore, without a doubt, the mean values of the IVIM-DWI parameters cannot adequately reflect the histological heterogeneity of tumor. Further studies that utilize texture or histogram analysis may be more meaningful in comprehensively understand the differences in the IVIM-DWI parametric values between AML and ccRCC.

In conclusion, our preliminary data indicates that AML and ccRCC differ significantly from each other in both the diffusion- and perfusion-related IVIM-DWI parametric values, which sug-gests that IVIM-DWI may sever as a supplementary tool in the differentiation between the most common tumors of kidney.

Disclosure of conflict of interest

None.

Abbreviations

ADC, apparent diffusion coefficient; AML, angiomyolipoma; ccRCC, clear cell renal cell carcinoma; D, pure diffusion coefficient; D*, pseudo-diffusion coefficient; f, perfusion fraction; IVIM-DWI, intravoxel incoherent motion diffusion-weighted imaging; RCC, renal cell carcinoma.

Address correspondence to: Dr. Xiaoping Yu, Department of Diagnostic Radiology, Hunan Cancer Hospital, The Affiliated Cancer Hospital of Xiangya School of Medicine, Central South University, No. 283 Tongzipo Road, Changsha 410013, P. R. China. Tel: +86-731-89762577; Fax: +86-731-89762577; E-mail: nj9015@163.com

References

[1] Motzer RJ, Agarwal N, Beard C, Bolger GB, Boston B, Carducci MA, Choueiri TK, Figlin RA, Fishman M, Hancock SL, Hudes GR, Jonasch E, Kessinger A, Kuzel TM, Lange PH, Levine EG, Margolin KA, Michaelson MD, Olencki T, Pili R, Redman BG, Robertson CN, Schwartz LH, Sheinfeld J and Wang J. NCCN clinical practice guidelines in oncology: kidney cancer. J Natl Compr Canc Netw 2009; 7: 618-630.

[2] Wen Z, Sun Z and Wang Y. Diagnostic utility of diffusion-weighted magnetic resonance imaging in two common renal tumors. Oncol Lett 2015; 10: 2565-2568.

[3] Xie P, Yang Z and Yuan Z. Lipid-poor renal angiomyolipoma: Differentiation from clear cell

renal cell carcinoma using wash-in and wash-out characteristics on contrast- enhanced computed tomography. Oncol Lett 2016; 11: 2327-2331.

[4] King KG, Gulati M, Malhi H, Hwang D, Gill IS, Cheng PM, Grant EG and Duddalwar VA. Quantitative assessment of solid renal masses by contrast-enhanced ultrasound with time-intensity curves: how we do it. Abdom Imaging 2015; 40:2461-2471.

[5] Ishigami K, Pakalniskis MG, Leite LV, Lee DK, Holanda DG and Rajput M. Characterization of renal cell carcinoma, oncocytoma, and lipid-poor angiomyolipoma by unenhanced, nephrographic, and delayed phase contrast- enhanced computed tomography. Clin Imaging 2015; 39: 76-84.

[6] Cornelis F, Tricaud E, Lasserre AS, Petitpierre F, Bernhard JC, Le Bras Y, Yacoub M, Bouzgarrou M, Ravaud A and Grenier N. Routinely performed multiparametric magnetic resonance imaging helps to differentiate common subtypes of renal tumours. Eur Radiol 2014; 24: 1068-1080.

[7] Mytsyk Y, Borys Y, Komnatska I, Dutka I and Shatynska-Mytsyk I. Value of the diffusion-weighted MRI in the differential diagnostics of malignant and benign kidney neoplasms - our clinical experience. Pol J Radiol 2014; 79: 290-295.

[8] Kim B, Lee SS, Sung YS, Cheong H, Byun JH, Kim HJ and Kim JH. Intravoxel incoherent motion diffusion-weighted imaging of the pancreas: characterization of benign and malignant pancreatic pathologies. J Magn Reson Imaging 2017; 45: 260-269.

[9] Yu XP, Wen L, Hou J, Bi F, Hu P, Wang H and Wang W. Discrimination between metastatic and nonmetastatic mesorectal lymph nodes in rectal cancer using intravoxel incoherent motion diffusion-weighted magnetic resonance imaging. Acad Radiol 2016; 23: 479-485.

[10] Gaing B, Sigmund EE, Huang WC, Babb JS, Parikh NS, Stoffel D and Chandarana H. Subtype differentiation of renal tumors using voxel-based histogram analysis of intravoxel incoherent motion parameters. Invest Radiol 2015; 50: 144-152.

[11] Le Bihan D, Breton E, Lallemand D, Aubin ML, Vignaud J and Laval-Jeantet M. Separation of diffusion and perfusion in intravoxel incoherent motion MR imaging. Radiology 1988; 168: 497-505.

[12] Zhang SX, Jia QJ, Zhang ZP, Liang CH, Chen WB, Qiu QH and Li H. Intravoxel incoherent motion MRI: emerging applications for nasopharyngeal carcinoma at the primary site. Eur Radiol 2014; 24: 1998-2004.

[13] Teloken PE, Thompson RH, Tickoo SK, Cronin A, Savage C, Reuter VE and Russo P. Prognos-

tic impact of histological subtype on surgically treated localized renal cell carcinoma. J Urol 2009; 182: 2132-2136.

[14] Chandarana H, Kang SK, Wong S, Rusinek H, Zhang JL, Arizono S, Huang WC, Melamed J, Babb JS, Suan EF, Lee VS and Sigmund EE. Diffusion-weighted intravoxel incoherent motion imaging of renal tumors with histopathologic correlation. Invest Radiol 2012; 47: 688-696.

[15] Vargas HA, Chaim J, Lefkowitz RA, Lakhman Y, Zheng J, Moskowitz CS, Sohn MJ, Schwartz LH, Russo P and Akin O. Renal cortical tumors: use of multiphasic contrast-enhanced MR imaging to differentiate benign and malignant histologic subtypes. Radiology 2012; 264: 779-788.

[16] Cornelis F, Tricaud E, Lasserre AS, Petitpierre F, Bernhard JC, Le Bras Y, Yacoub M, Bouzgarrou M, Ravaud A and Grenier N. Routinely performed multiparametric magnetic resonance imaging helps to differentiate common subtypes of renal tumours. Eur Radiol 2014; 24: 1068-1080.

[17] Le Bihan D and Turner R. The capillary network: a link between IVIM and classical perfusion. Magn Reson Med 1992; 27: 171-178.

[18] Lee HJ, Rha SY, Chung YE, Shim HS, Kim YJ, Hur J, Hong YJ and Choi BW. Tumor perfusion-related parameter of diffusion-weighted magnetic resonance imaging: correlation with histological microvessel density. Magn Reson Med 2014; 71: 1554-1558.

[19] Sumi M, Van Cauteren M, Sumi T, Obara M, Ichikawa Y and Nakamura T. Salivary gland tumors: use of intravoxel incoherent motion MR imaging for assessment of diffusion and perfusion for the differentiation of benign from malignant tumors. Radiology 2012; 63: 770-777.

[20] Lemke A, Laun FB, Simon D, Stieltjes B and Schad LR. An in vivo verification of the intravoxel incoherent motion effect in diffusion-weighted imaging of the abdomen. Magn Reson Med 2010; 64: 1580-1585.

[21] Taouli B, Thakur RK, Mannelli L, Babb JS, Kim S, Hecht EM, Lee VS and Israel GM. Renal lesions: characterization with diffusion-weighted imaging versus contrast- enhanced MR imaging. Radiology 2009; 251: 398-407.

[22] Agnello F, Roy C, Bazille G, Galia M, Midiri M, Charles T and Lang H. Small solid renal masses: characterization by diffusion-weighted MRI at 3 T. Clin Radiol 2013; 68: e301-308.

[23] Tanaka H, Yoshida S, Fujii Y, Ishii C, Tanaka H, Koga F, Saito K, Masuda H, Kawakami S and Kihara K. Diffusion-weighted magnetic resonance imaging in the differentiation of angiomyolipoma with minimal fat from clear cell renal cell carcinoma. Int J Urol 2011; 18: 727-730.

[24] Zhang H, Gan Q, Wu Y, Liu R, Liu X, Huang Z, Yuan F, Kuang M and Song B. Diagnostic performance of diffusion-weighted magnetic resonance imaging in differentiating human renal lesions (benignity or malignancy): a meta-analysis. Abdom Radiol (NY) 2016; 41: 1997-2010.

[25] Sasamori H, Saiki M, Suyama J, Ohgiya Y, Hirose M and Gokan T. Utility of apparent diffusion coefficients in the evaluation of solid renal tumors at 3T. Magn Reson Med Sci 2014; 13: 89-95.

[26] Xu X, Wang P, Ma L, Shao Z, Shao Z and Zhang M. Diffusion weighted imaging and perfusion weighted imaging in the differential diagnosis of benign and malignant renal masses on 3.0 T MRI. Zhonghua Yi Xue Za Zhi 2015; 95: 200-204.